Diurnal Cycle of Summertime Deep Convection over North America: A Satellite Perspective

Baijun Tian

Atmospheric and Oceanic Sciences Program,
Princeton University, Princeton, NJ

Isaac M. Held, Ngar-Cheung Lau, and Brian J. Soden

NOAA Geophysical Fluid Dynamics Laboratory,
Princeton, NJ

Submitted to J. Geophys. Res. - Atmosphere

07/23/2004

Corresponding author address: Baijun Tian, GFDL, Princeton University, P. O. Box 308, Princeton, NJ 08542. Tel: 1-609-452-6566. Fax: 1-609-987-5063. Email: Baijun.Tian@noaa.gov

Abstract

High-resolution (0.1°x0.1°) geostationary satellite infrared radiances at 11 μm in combination with gridded (2.5°x2.0°) hourly surface precipitation observations are employed to document the spatial structure of the diurnal cycle of summertime deep convection and associated precipitation over North America. Comparison of the diurnal cycle pattern between the satellite retrieval and surface observations demonstrates the reliability of satellite radiances for inferring the diurnal cycle of precipitation, especially the diurnal phase. Based on the satellite radiances, we find that over most land regions, deep convection peaks in the late afternoon and early evening, consistent with the strong diurnal cycle of land surface temperature. However, strong regional variations exist in both the diurnal phase and amplitude, implying that topography, land-sea contrast, and coastline curvature play an important role in modulating the diurnal cycle. Examples of such affects are highlighted over Florida, the Great Plains, and the North America monsoon region.

1. Introduction

The diurnal cycle of tropical deep convection and associated precipitation is of intrinsic interest with studies dating back several decades (e.g., Wallace 1975; Gray and Jacobson 1977; Yang and Slingo 2001). The studies using global data sets indicate that there is a clear land–sea contrast in the diurnal cycle of tropical convection (e.g., Yang and Slingo 2001; Tian et al. 2004). Over land, the diurnal variation is strong, and maximum convection occurs in the late afternoon and early evening. In contrast, it is relatively weak over the oceans with peaks in the morning. While the physical mechanisms behind the oceanic diurnal cycle are still unclear, the diurnal cycle of continental convection can be mainly attributed to a direct thermodynamic response to the strong diurnal cycle of solar heating land surface temperature, and atmospheric stability (Wallace 1975; Yang and Slingo 2001; Tian et al. 2004).

However, strong regional variations in diurnal cycle are found over many inland and coastal regions of the world, highlighting the importance of land-sea breeze and mountain-valley wind as well as coastline curvature in modulating the diurnal cycle (e.g., Yang and Slingo 2001; Ohsawa et al. 2001; Mapes et al. 2003; Zuidema 2003). For example, Yang and Slingo (2001) suggested that the diurnal phase and amplitude over Africa and South America is in part modulated by the local orography. They also noted that the strong diurnal signal over land is spread out over the adjacent oceans, such as the Bay of Bengal, probably through gravity waves of varying depths. Through investigating the physical processes related to the rainfall climate over the Panama Bight and Pacific littoral of Colombia, Mapes et al. (2003) described how the mesoscale structure of the diurnal cycle in that region is controlled by the complex coastlines and topography.

Complex topography and coastlines are also found over North America (NA) (Fig. 1), such as the orography contrast between the Rocky Mountains and the Great Plains, and coastline

curvature around the Florida peninsula. And in northwestern Mexico, the core NA monsoon (NAM) region, the mountains of the Sierra Madre Occidental (SMO) are located near the coast, next to the Gulf of California (GC), resulting in both strong mountain-valley and land-sea contrasts in this region. Thus, detailed mesoscale structures in the diurnal cycle over NA are expected. As a result, high spatial and temporal resolution data that are able to resolve the land-sea contrast, coastline curvature, mountains and valleys are required to study the diurnal cycle over NA.

Most previous studies on the diurnal cycle over NA have relied on a gridded, 2.5° longitude by 2.0° latitude, hourly precipitation data set produced by Higgins et al. (1996) from quality-controlled station records over the United States (US) (e.g., Higgins et al. 1997; Dai et al. 1999). Other studies relied directly on surface station records over limited regions of the US (e.g., Wallace 1975; Schwartz and Bosart 1979; Riley et al. 1987; Landin and Bosart 1989). In particular, due to the sparse quality surface station data over Mexico, the diurnal cycle of the NAM precipitation is poorly documented. Negri et al. (1993; 1994) presented the warm season rainfall for the southwest US and Mexico derived from high spatial resolution Special Sensor Microwave Imager (SSM/I) and examined the diurnal cycle. However, due to the limitation of the polar-orbiting satellites, the morning and evening overpass times cannot fully resolve the diurnal cycle in these studies. In summary, due mainly to the lack of high spatial and temporal resolution surface or satellite data, the spatial structure of the diurnal cycle over NA has not been fully explored by the previous studies. This is particularly true over the NAM region, even though most of the rainfall in this region is diurnal (US CLIVAR Pan American Implementation Panel 2002; Higgins et al. 2004). The IR radiances at the 11 μm channel from geostationary satellites offer unmatched spatial and temporal resolutions and have been widely applied to study the diurnal cycle of tropical deep convection and precipitation (e.g., Meisner and Arkin 1987;

Yang and Slingo 2001; Mapes et al. 2003; Tian et al. 2004), making it an ideal data source for studying the spatial structure of the diurnal cycle over NA.

The purposes of this study are two-fold: First, we assess the reliability of satellite radiances for inferring the diurnal cycle of precipitation by comparing satellite retrievals with surface precipitation observations, which are both available over the US for the year 1999. Second, relying on the high-resolution (0.1°x0.1°, 3-hourly) satellite radiances, we document the spatial structure of the diurnal cycle of summertime deep convection and precipitation over NA. The outline for the rest of this paper is as follows: The satellite radiances, method of precipitation retrieval from radiances, surface precipitation observations, and diurnal cycle analysis method are described in section 2. Section 3 will present a comparison of the diurnal cycles between satellite retrievals and surface observations over the US for 1999. We also compare the diurnal cycle for 1999 with a 20-year average from 1982 to 2001, based on the surface observations over the US in section 4. The diurnal cycle of summertime deep convection over NA based on the high-resolution satellite radiances, are shown in section 5. Conclusions are summarized in section 6.

2. Data and Method

The primary data for this study are geostationary satellite IR radiances (expressed as equivalent black body temperatures) in the window (11 μm) channel (T_{11}) from GOES-10 (180°-105°W) and GOES-8 (105°W-35°W). The data cover the year 1999 at a temporal resolution of 3 hours and a spatial resolution of 0.1°×0.1° longitude-latitude. Details regarding radiance measurements and satellite inter-calibration can be found in Tian et al. (2004). The independent surface precipitation observations for this study are from the updated Higgins et al. (1996), a

gridded hourly precipitation data set constructed from quality-controlled surface station records over the US, covering the period from 1943 to 2002 and with resolution 2.5° longitude by 2.0° latitude.

To retrieve precipitation from the satellite radiances, we rely on the simplest GOES precipitation index (GPI) originally developed by Arkin and Meisner (1987) as follows,

$$GPI = aF_c \tag{1}$$

F_c is the fractional coverage of deep convective clouds (T_{11} < 230K) within a large-scale grid box (2.5° longitude by 2.0° latitude) or a high-resolution pixel (0.1°×0.1° longitude-latitude).In the latter case, F_c equals either 100% or 0, and a long time average is required, such as a season in our case, in order for the GPI to be meaningful. a is a constant factor 3 mm h^{-1} within the Tropics (25°S–25°N) and linearly decreases poleward due to the zenith angle dependence of the satellite radiances (Joyce and Arkin 1997).

Fig. 2 shows the summertime mean precipitation over the US with resolution 2.5° longitude by 2.0° latitude based on satellite radiances for 1999 (a), surface observations for 1999 (b), and surface observations for the climatology (c). Comparing the surface-observed mean precipitation for 1999 (Fig. 2b) with the 20-year average (Fig. 2c) indicates that the general precipitation pattern over the US in 1999 is consistent with the longer-term climatology although it is relatively drier over the northern parts of the country. Comparing the precipitation between satellite retrieval (Fig. 2a) and surface observations (Fig. 2b) for 1999 indicates that the satellite retrieval is comparable to the surface observations in magnitude and spatial pattern. Both data sets show that strong precipitation is found over Florida and Midwest, while dry conditions are common over western and northeastern US. However, significant difference is found over the Great Plains, where the satellite retrieval is twice as large as surface observation. This difference

may be due to the deficiency of the simplest GPI algorithm and/or different sampling locations for satellite and surface observations. For example, the condensation associated with the deep convective clouds over this region may be re-evaporated before falling to the ground, causing the deep convective cloud index to exceed the observed rainfall at the surface. A similar difference between microwave retrieval and surface observations is found for the US (Eric Wilcox, personal communication). This systematic bias in the mean will result in systematic bias in diurnal magnitude over the Great Plains but should not be a serious problem for diurnal phase.

It is worth noting that our usage of GPI in this study has pushed the GPI beyond its realm of calibrated validity by calculating precipitation at high-resolution (0.1°x0.1°), in mid-latitudes, and at different times of day. Because of this concern, Garreaud and Wallace (1997) omitted the 3 mm h^{-1} factor in their climatology of T11< 235 K cloudiness. We prefer the rain-rate units as in Mapes et al. (2003) for the sake of easy discussion and also prefer this simple 3 mm h^{-1} factor to more complex calibrations because of the uncertainties involved.

For the diurnal cycle analysis, we first calculate the June, July, and August three-month average hourly (surface) or 3-hourly (satellite) precipitation at each grid or pixel. The resulting diurnal composite of precipitation is then decomposed spectrally using a Fourier transform to obtain the diurnal amplitude and phase following Tian et al. (2004).

3. Are Satellite IR Radiances Reliable for Inferring the Diurnal Cycle of Precipitation?

Although the satellite radiances have been widely applied to study the diurnal cycle of tropical precipitation, the reliability of this approach has not been verified by independent surface observations. In this section, we compare the summertime precipitation and its diurnal cycle over the US derived from the satellite radiances and surface observations to assess the reliability of this approach. Fig. 3 shows the diurnal amplitudes and phases over the US with

resolution 2.5° longitude by 2.0° latitude based on satellite radiances for 1999 (a), surface observations for 1999 (b), and surface observations for the climatology (c). The diurnal amplitude is denoted by the color shading and also by the length of the arrow (see key on inset in Fig. 3). The diurnal phase can be determined from the orientation of the arrows with respect to a 24-hour clock. Arrows pointing upward indicate a peak at 0000 local solar time (LST) (midnight), downward indicate a peak at 1200 LST (noon), towards the right indicate a peak at 0600 LST (dawn), and towards the left a peak at 1800 LST (sunset).

Comparing the diurnal cycles between satellite retrievals (Fig. 3a) and surface observations (Fig. 3b) for 1999 indicates that the diurnal pattern from the satellite retrievals is in broad agreement with surface observations. For example, both data sets show late afternoon maxima over the eastern, southeastern, and western US including the Rocky Mountains and near midnight maxima over the Great Plains. Both data sets also agree on the regions of significant diurnal amplitude, such as the southeastern US, especially Florida, and the Great Plains. The diurnal amplitudes are also comparable over most regions, except for the Great Plains, where the diurnal amplitudes from satellite retrievals are systematically larger than those from surface observations. This is due to the systematic biases of the GPI algorithm in the mean precipitation over the Great Plains (Fig. 2). Nonetheless, the broad agreement in the diurnal pattern from satellite retrievals and surface observations demonstrates that satellite radiances are reliable for inferring the diurnal cycle of precipitation, especially the diurnal phase.

4. Is One Season Long Enough to Represent the Diurnal Cycle Climatology?

Since the satellite radiances are only available to us for 1999, one might wonder whether one season is long enough to represent the diurnal cycle climatology. To address this concern, we also compare the surface-observed diurnal cycle for 1999 with a 20-year average over the

period 1982 to 2001. Consistent with previous studies (e.g., Higgins et al. 1997; Dai et al. 1999), the climatological summertime precipitation diurnal cycle from surface observations (Fig. 3c) is characterized by late afternoon maxima over the eastern, southeastern, and western US including the Rocky Mountains and near midnight maxima over the Great Plains and Midwest. Significant diurnal amplitudes are found over the southeastern US, especially Florida, and the Great Plains. Comparing the diurnal cycle for 1999 (Fig. 3b) with the climatology (Fig. 3c) indicates that the dominant features of the diurnal cycle over the US in 1999 is consistent with the climatology, suggesting that one season of satellite data is sufficient to investigate the diurnal cycle at higher resolution.

5. Diurnal Cycle of Summertime Deep Convection and Precipitation over NA

In Fig. 4, we present the diurnal cycle of summertime convection and precipitation over NA at the spatial resolution 0.1° longitude by 0.1° latitude relying on the satellite radiances. For clarity, the arrows are plotted every 7 pixels with the arrows greater than 4 mm day^{-1} all having the same length, and the arrows less than 0.5 mm day^{-1} omitted. Fig. 4 indicates that the prominent feature of the diurnal cycle over NA is a land–sea contrast, consistent with the general characteristics of the diurnal cycle of tropical deep convection. Over the oceans, such as Pacific Ocean, the Gulf of Mexico, and Atlantic Ocean, the diurnal cycle is weak with peaks near noon. Over most land regions, the deep convection tends to peak in the late afternoon and early evening with strong diurnal amplitudes, consistent with the thermodynamic response to the strong diurnal cycle of the land surface temperature. However, there are strong regional variations in both diurnal phases and amplitudes over land, suggesting that topography, land-sea contrast, and coastline curvature play an important role in modulating the diurnal cycle pattern. For example, near midnight maxima are found over the Great Plains, evidently associated with

the eastern slope of the Rocky Mountains. The strong diurnal variation of the NAM rainfall, the largest diurnal amplitude over all of NA, is concentrated over the western slopes of the SMO. Furthermore, regional maxima in diurnal amplitudes are found over the Florida peninsula, the Yucatan peninsula, and the island of Cuba due to land-sea contrast and coastline curvature. Over the western US, the diurnal amplitudes are generally small. In general, the regions of large diurnal amplitudes are also the regions of large daily mean convection, consistent with the general characteristics of the diurnal cycle of tropical deep convection (e.g., Tian et al. 2004). It is also interesting to note that the boundary between the late afternoon maxima over the western US and the near midnight maxima over the Great Plains is the Continental Divide (106ºW). Moreover, the boundary between the near midnight maxima over the Great Plains and the late afternoon maxima over the eastern and southeastern US approximately follows the 200-m elevation line (Figs. 1 and 4), running from southwest to northeast in the central US. Along this boundary, the diurnal amplitudes are generally small.

Over the coast of the Gulf of Mexico, the Florida peninsula, the Yucatan peninsula, and the island of Cuba, the convection and its diurnal cycle are strong with peaks in the late afternoon (1600-1800 LST). Over Florida, the maximum diurnal amplitude (around 9 mm day^{-1}) is found just southwest of the Lake Okeechobee over south Florida and the diurnal amplitude decreases from south to north and from inland peninsula to the coastal regions. Furthermore, the diurnal phase is earlier (around 1600 LST) over south Florida and shifts later to the north (around 1800 LST over Georgia and Alabama). Our results of the diurnal cycle over Florida are in broad agreement with previous observational studies based on surface station data, such as Schwartz and Bosart (1979). We note that phase also shifts over the island of Cuba, from 1800 LST at the eastern tip to 1500 LST to the western tip. The phase then shifts back to 1800 LST as one moves over the Yucatan. The physical mechanisms responsible for the strong diurnal cycle over the

coast of the Gulf of Mexico, the Florida peninsula, the Yucatan peninsula, and the island of Cuba are relatively well understood. It is generally accepted that the stronger diurnal cycle over most tropical/subtropical coastal areas, such as the coasts of the Gulf of Mexico, than in most inland regions is the result of sea breeze fronts (e.g., Atkinson 1981; Pielke and Segal 1986; Pielke 2001). It is also generally accepted that the stronger diurnal cycle over most tropical/subtropical islands or peninsulas, such as Florida, Yucatan, and Cuba, than in most coastal areas is due to the low-level convergence caused by sea breezes entering the islands or peninsulas from coasts (e.g., Houze et al. 1981; Yang and Slingo 2001). This mechanism for the strong diurnal cycle over south Florida was initially pointed out by Byers and Rodebush (1948) and further validated by observational study by Burpee (1979) and three-dimensional numerical model simulation of the sea breezes by Pielke (1974).

Fig. 5 shows the diurnal cycle over the Rocky Mountains and the Great Plains, plotted every 3 pixels. The solid contours are surface elevation. Over the Rocky Mountains, west of the Continental Divide (106°W), the convection and its diurnal cycle are weak with a peak at 1800 LST. In contrast, the diurnal cycle is strong with near a midnight maximum over the Great Plains, consistent with previous studies based on the surface station data, such as Riley et al. (1987) and Dai et al. (1999), and studies based on radar observations by Carbone et al. (2002). Our high-resolution satellite data depict smooth transitions in the diurnal phase from late afternoon to early morning as the elevation decreases eastward from the Rocky Mountains to the Great Plains. Although near midnight maximum of convection over the Great Plains is a well-known fact with studies dating back several decades, the physical mechanisms that are responsible for this phenomenon are still not completely understood. The mechanisms proposed before 1975 have been summarized by Wallace (1975), who grouped them into two categories: those based on thermodynamical processes that affect the static stability, and those based on

dynamical processes that influence the mass convergence within the planetary boundary layer. The proposed thermodynamic mechanisms include radiative cooling from cloud tops and low-level warm advection. The proposed dynamic processes include the nocturnal low-level jet (LLJ) over the Great Plains (Pitchford and London 1962; Bonner 1968) and related changes in frictional drag associated with diurnal variation of static stability (Blackadar 1957). The relationship between the nocturnal LLJ and the nocturnal maxima of convection at the Great Plains remains a topic of current research (e.g., Helfand and Schubert 1995; Higgins et al. 1997). After 1975, a new mechanism was proposed by Riley et al. (1979), who argued that the diurnal phase transitions of precipitation are highly suggestive of the convective precipitation systems forming in the mountains during the late afternoon and then spreading eastward onto the Great Plains. Recently, using radar observations Carbone et al. (2002) documented the eastward-propagation of precipitation systems.

The smooth diurnal phase shifts in our results demonstrate the spatial and temporal continuities of the diurnal cycle over the Great Plains. They are also support the Riley et al. (1987) mechanism. To further demonstrate this point, the Hovmöller (time-longitude) diagram of satellite radiances averaged over 40–41ºN for 15–25 June 1999 is shown in Fig. 6. Eastward propagating convective systems are a prominent feature east of the Continental Divide, in stark contrast to the prevailing stationary convection over the mountains. The eastward propagating convective systems are generally initiated at or near the east slope of the Continental Divide (around 106ºW) in the late afternoon and then propagate down the slope eastward and reach the Great Plains at night as in Carbone et al. (2002). The propagation speed is about 15 m s^{-1}, often in excess of rates that are attributable either to the phase speeds of large-scale forcing or to advection from low- to midlevel "steering" winds as pointed out by Carbone et al. (2002), who speculated that wavelike mechanisms, in the free troposphere and/or the planetary boundary

layer, might contribute to the rates of motion observed (see also Yang and Slingo 2001; Mapes et al. 2003). Toth and Johnson (1985) also documented an eastward propagation of the upslope-to-downslope surface transition zones across the Plains, which may also be responsible for this eastward propagation of convective systems.

Afternoon convection is rare over the Great Plains. This is likely at least in part a result of daytime upslope wind blowing from the Great Plains to the Rockies, driven by the strong diurnal cycle of the mountain surface temperature and the sloping terrain of the Great Plains. Daytime upslope and nocturnal drainage flow (e.g., Atkinson 1981; Pielke and Segal 1986; Pielke 2001) is also a classic mesoscale atmospheric circulation, although less extensively studied compared to the land-sea breeze. Toth and Johnson (1985) found that the daytime flow over the Front Range of Colorado was dominated by a thermally induced easterly upslope flow (their Fig. 10). Higgins et al. (1997) also showed an afternoon easterly upslope wind over Texas based on reanalysis (their Fig. 10). The upward velocities associated with the upslope winds provide in the mountains an additional triggering mechanism for convection initiation in the afternoon. On the other hand, the downward return flow of the upslope wind suppresses the convection over the Great Plains in the afternoon, which may offset the diurnal forcing of the local surface temperature. In summary, the near midnight maxima of convection over the Great Plains result from the combination of a suppression of afternoon convection and the nighttime arrival of the eastward propagating convective systems, which are initiated at the Rocky Mountains in the previous afternoon.

The mean precipitation and its diurnal cycle (plotted every 3 pixels) over the core NAM region are shown in Fig. 7. The strong precipitation and diurnal cycle are concentrated over the western slopes of the SMO and run from northwest to southeast closely following the terrain lines with maxima at the elevation of around 1200 meters. The precipitation and its diurnal cycle

decrease rapidly both westward to the GC and eastward to the mountain peak and the east side of the SMO. On the west slopes of the SMO, the convection tends to peak around late afternoon and early evening (1800-2200 LST), while late afternoon (1800 LST) convection is dominant over the eastern side of the SMO. Over the GC, nocturnal convection is common but with weak amplitudes. However, over the mouth of the GC (~20−24°N), the coastline is concave seaward and the spatial structures of convection and its diurnal cycle are different from the GC. Fig. 8a indicates that strong convection is located not only onshore but also offshore. As a result, the maximum convection (12 mm day^{-1}) is located at the coast (105ºW, 21.5ºN) instead of further inland. This is the most intense convection over the NAM region (Fig. 7a). The spatial structure of the diurnal cycle over the mouth of the GC is particularly interesting and is shown in Fig. 8, with arrows plotted every pixel. A significant diurnal cycle is found offshore in contrast to the small diurnal amplitudes over the GC. The diurnal amplitude decreases as one moves farther away from land. The land-sea contrast in diurnal phase is clear, with evening maximum onshore and morning maximum offshore; however, the transition at the coastline in not abrupt. Rather, the diurnal phase shifts very smoothly from evening at the coastal lands to early morning at the coastal waters then to late morning farther offshore. The speed of the diurnal seaward sweep of convection is around 10 m s^{-1}. In general, our results are consistent with the studies by Negri et al. (1993; 1994) based on SSM/I but with important new information.

The strong late afternoon and early evening convection over the western slopes of the SMO is easily understood and generally regarded as a result of the mountain lifting of a vigorous sea and valley breeze (e.g., Negri et al. 1994; Strensrud et al. 1995; Berbery 2001). The presence of mountains next to coast usually results in a circulation that blends the sea/land breeze and mountain/valley wind. Numerical simulations indicate that the combined circulation is much more intense than when they act separately (e.g., Mahrer and Pielke 1977). This mountain lifting

of the sea and valley breeze is an important initiation mechanism for afternoon convection over coastal mountains. The physical mechanisms responsible for the morning convection over the coastal waters are less clear. Traditionally, the offshore morning convection has been attributed to the offshore convergence of land/mountain breezes (e.g., Houze et al. 1981; Negri et al. 1994). For example, if a land breeze meets a low-level prevailing flow offshore (e.g., Ramage 1965; Kousky 1980; Houze et al. 1981) or the coastline is concave seaward (e.g., Negri et al. 1994; Ohsawa et al. 2001; Zuidema 2003), the land breezes will tend to convergence offshore, which will initiate deep convection over the coastal waters. Since the Mexican coastline is concave seaward over the mouth of the GC, the offshore convergence of the nocturnal drainage flows and land breezes from the SMO to the GC may be responsible for the offshore morning convection found here. However, Mapes et al. (2003) has argued that nighttime radiative cooling of land and the associated thermal land breezes are much weaker than the corresponding daytime sea breezes, especially under humid tropical skies. Most importantly, the convergence of land breezes cannot explain the graduate diurnal phase shift in the satellite data (Fig. 8). Thus, the land breeze convergence may not be the complete explanation of nocturnal convection in coastal areas.

Similar to the Great Plains, the smooth diurnal phase shifts over the mouth of the GC demonstrate the spatial and temporal continuities of the diurnal cycle over this region. They also indicate that the morning convection over the waters may be developed over the coastal mountains in the previous evening. To demonstrate this point, the Hovmöller (time-longitude) diagram of satellite radiances averaged over 21.5−22.5ºN for 5−10 August 1999 is shown in Fig. 9. Note the coastline is located around 105.5ºW. Westward (seaward) propagating convective systems are the dominant features over this region. The convective systems are generally initiated in the evening at the coastal mountains, in response to the diurnal heating of mountain

surface temperature and then propagate westward over the oceans after midnight and gradually dissipate. These westward propagating systems can explain the morning convection, the smooth diurnal phase and diurnal amplitude decrease over the waters (Fig. 8). The seaward propagating convective systems may be a result of a seaward propagating diurnal gravity wave in the planetary boundary layer radiating from the coastal mountain mixed layer as proposed by Yang and Slingo (2001) and Mapes et al (2003).

6. Conclusions

The principal findings of this study are:

1) Comparing the diurnal cycle over the US between satellite retrievals and surface observations indicates that the diurnal pattern from the satellite retrievals is in broad agreement with surface observations. This demonstrates that satellite radiances are reliable for inferring the diurnal cycle of precipitation, especially the diurnal phase.

2) Comparing the surface-observed diurnal cycle over the US for 1999 with a 20-year average indicates that one season is long enough to represent the diurnal cycle climatology.

3) Over most land regions, deep convection peaks in the late afternoon and early evening. However, strong regional variations exist in both diurnal phase and amplitude over NA, implying that topography, land-sea contrast, and coastline curvature play an important role in modulating the diurnal cycle.

4) Over the coast of the Gulf of Mexico, the Florida peninsula, the Yucatan peninsula, and the island of Cuba, the convection and its diurnal cycle are strong with peaks in the late afternoon (1600−1800 LST). Over Florida, the maximum diurnal amplitude (around 9 mm day^{-1}) is found just southwest of the Lake Okeechobee over south Florida and the diurnal amplitude decreases from south to north and from inland peninsula to the coastal regions. Furthermore, the

diurnal phase is earlier (around 1600 LST) over south Florida and shifts later to the north (around 1800 LST over Georgia and Alabama).

5) Near midnight maxima of convection are found over the Great Plains with smooth transitions in the diurnal phase from late afternoon to early morning over the Great Plains. Satellite data also demonstrate that the near midnight convection over the Great Plains are the result of the eastward propagating convective systems initiated at the Rocky Mountains in the previous afternoon.

6) Over the northwestern Mexico, strong precipitation and diurnal cycle are concentrated over the western slopes of the SMO and run from northwest to southeast closely following the terrain lines with maxima at the elevation of around 1200 meters. The diurnal cycle decreases rapidly both westward to the GC and eastward to the mountain peak. On the west slopes of the SMO, the convection peaks around late afternoon and early evening (1800-2200 LST), while late afternoon (1800 LST) convection is dominant over the eastern side of the SMO. Over the GC, nocturnal convection is common but with weak amplitudes. However, over the mouth of the GC, significant diurnal cycles are found offshore with amplitude decreasing from coastal waters farther offshore. Furthermore, the diurnal phase shifts smoothly from early morning at the coastal waters to late morning farther offshore. Satellite data demonstrate that the morning convection offshore is the result of the westward propagating convective systems initiated at the coastal mountains in the previous evening.

Acknowledgements

We wish to thank Xiangqian Wu for providing us the satellite data, Siegfried D. Schubert, Myong-In Lee and Hyun-Kyung Kim for providing the surface precipitation data and their assistance in analyzing the data, as well as Keith Dixon for providing the 20-minute surface

relief data. Discussions with Jeff Ploshay and the GFDL internal reviews from Eric M. Wilcox and Stephen T. Garner are appreciated. This research was supported in part by ARM grant DE-AI02-00ER62900.

References

Arkin, P. A., and B. N. Meisner, 1987: The relationship between large-scale convective rainfall and cold cloud over the western hemisphere during 1982-84. *Mon. Wea. Rev.*, **115**, 51-74.

Atkinson, B. W., 1981: *Meso-scale Atmospheric Circulations*. Academic Press, 495 pp.

Blackadar, A. K., 1957: Boundary layer wind maxima and their significance for the growth of nocturnal inversions. *Bull. Amer. Meteor. Soc.*, **38**, 283-290.

Berbery, E. H., 2001: Mesoscale moisture analysis of the North American Monsoon. *J. Climate*, **14**, 121-137.

Bonner, W. D., 1968: Climatology of the low level jet. *Mon. Wea. Rev.*, **96**, 833-850.

Burpee, R. W., 1979: Peninsula-scale convergence in the South Florida sea breeze. *Mon. Wea. Rev.*, **107**, 852-860.

Byers, H. R., and H. R. Rodebush, 1948: Causes of thunderstorms of the Florida peninsula. *J. Meteor.*, **6**, 275-280.

Carbone, R. E., J. D. Tuttle, D. A. Ahijevych, and S. B. Trier, 2002: Inferences of predictability associated with warm season precipitation episodes. *J. Atmos. Sci.*, **59**, 2033-2056.

Dai, A., F. Giorgi, and K. E. Trenberth, 1999: Observed and model-simulated diurnal cycles of precipitation over the contiguous United States. *J. Geophys. Res.*, **104**, 6377-6402.

Garreaud, R. D., and J. M. Wallace, 1997: The diurnal march of convective cloudiness over the Americas. *Mon. Wea. Rev.*, **125**, 3157-3171.

Helfand, H. M., and S. D. Schubert, 1995: Climatology of the Great Plains low-level jet and its contribution to the continental moisture budget of the United States. *J. Climate*, **8**, 784-806.

Higgins, R. W., J. E. Janowiak, and Y. Yao, 1996: *A Gridded Hourly Precipitation Data Base for the United States (1963-1993)*. NCEP/Climate Prediction Center Atlas, Vol. 1, Natl. Weather Serv., Camp Springs, MD, 47 pp.

Higgins, R. W., Y. Yao, E. S. Yarosh, J. E. Janowiak, and K. C. Mo, 1997: Influence of the Great Plains low-level jet on summertime precipitation and moisture transport over the central United States. *J. Climate*, **10**, 481-507.

Higgins, R. W., et al. 2004: The North American Monsoon Experiment (NAME) Science and Implementation Plan. Available online at http://www.cpc.ncep.noaa.gov/products/precip/monsoon/NAME.html.

Houze, R. A. Jr., S. G. Geotis, F. D. Marks Jr., and A. K. West, 1981: Winter monsoon convection in the vicinity of north Borneo. Part I: Structure and time variation of the clouds and precipitation. *Mon. Wea. Rev.*, **109**, 1595-s1614.

Joyce, R., and P. A. Arkin, 1997: Improved estimates of tropical and subtropical precipitation using the GOES Precipitation Index. *J. Atmos. Oceanic Technol.*, **14**, 997-1011.

Kousky, V. E., 1980: Diurnal rainfall variation in Northeast Brazil. *Mon. Wea. Rev.*, **108**, 488-498.

Landin, M. G. and L. F. Bosart, 1989: The diurnal variation of precipitation in California and Nevada. *Mon. Wea. Rev*., **117**, 1801-1816.

Mahrer, Y., and R. A. Pielke, 1977: The effects of topography on sea and land breezes in a two-dimensional numerical model. *Mon. Wea. Rev.*, **105**, 1151-1162.

Mapes, B. E., T. T. Warner, M. Xu, and A. J. Negri, 2003: Diurnal patterns of rainfall in Northwestern South America. Part I: Observations and context. *Mon. Wea. Rev.*, **131**, 799-812.

Mapes, B. E., T. T. Warner, and M. Xu, 2003: Diurnal patterns of rainfall in Northwestern South America. Part III: Diurnal gravity waves and nocturnal convection offshore. *Mon. Wea. Rev.*, **131**, 830-844.

Meisner, B. N. and P. A. Arkin, 1987: Spatial and annual variations in the diurnal cycle of large-scale tropical convective cloudiness and precipitation. *Mon. Wea. Rev.*, **115**, 2009-2032.

Negri, A. J., R. Adler, R. A. Maddox, K. W. Howard, and P. R. Keehn, 1993: A regional rainfall climatology over Mexico and the southwest United States derived from passive microwave and geosynchronous infrared data. *J. Climate*, **6**, 2144-2161.

Negri, A. J., R. F. Adler, E. J. Nelkin, and G. J. Huffman, 1994: Regional rainfall climatologies derived from Special Sensor Microwave Imager (SSM/I) data. *Bull. Amer. Meteor. Soc.*, **75**, 1165-1182.

Ohsawa, T., H. Ueda, T. Hayashi, A. Watanabe, and J. Masumoto, 2001: Diurnal variations of convective activity and rainfall in tropical Asia. *J. Meteor. Soc. Japan*, **79**, 333-352.

Pielke, R. A., and M. Segal, 1986: Mesoscale circulations forced by differential terrain heating. *Mesoscale Meteorology and Forecasting*, P. S. Ray, Ed., Amer. Meteor. Soc., 516-548.

Pielke, R. A., 2001: *Mesoscale Meteorological Modeling*. 2nd Edition, Academic Press, Inter. Geophys. Ser. 78, 676 pp.

Pitchford, K. L., and J. London, 1962: The low-level jet as related to nocturnal thunderstorms over Midwest United States. *J. Appl. Meteor.*, **1**, 43-47.

Ramage, C. S., 1965: Diurnal variation of summer rainfall over Malaya. *J. Trop. Geogr*, **19**, 62-68.

Riley, G. T., M. G. Landin, and L. F. Bosart, 1987: The diurnal variability of precipitation across the Central Rockies and adjacent Great Plains. *Mon. Wea. Rev.*, **115**, 1161-1172.

Schwartz, B. E. and L. F. Bosart, 1979: The diurnal variability of Florida rainfall. *Mon. Wea. Rev.*, **107**, 1535-1545.

Stensrud, D. J., R. L. Gall, S. L. Mullen, and K. W. Howard, 1995: Model climatology of the Mexican Monsoon. *J. Climate*, **8**, 1775-1794.

Tian, B., B. J. Soden, and X. Wu, 2004: Diurnal cycle of convection, clouds, and water vapor in the tropical upper troposphere: Satellites versus a general circulation model. *J. Geophys. Res.*, **109**, D10101, doi:10.1029/2003JD004117.

Toth, J. J., and R. H. Johnson, 1985: Summer surface flow characteristics over northeast Colorado. *Mon. Wea. Rev.*, **113**, 1458-1469.

U.S. CLIVAR Pan American Implementation Panel, 2002: *U.S. CLIVAR Pan American Research: A Scientific Prospectus and Implementation Plan*, U.S. CLIVAR Office, Washington, DC, 58 pp.

Wallace, J. M., 1975: Diurnal variations in precipitation and thunderstorm frequency over the conterminous United States. *Mon. Wea. Rev*., **103**, 406-419.

Yang, G.-Y., and J. M. Slingo, 2001: The diurnal cycle in the Tropics. *Mon. Wea. Rev*., **129**, 784-801.

Zuidema, P., 2003: Convective clouds over the Bay of Bengal. *Mon. Wea. Rev.*, **131**, 780-798.

Figure Captions

Figure 1: The 20-minute surface elevation over NA

Figure 2: The summertime mean precipitation over the US with resolution 2.5° longitude by 2.0° latitude based on satellite data for 1999 (2a), surface data for 1999 (2b), and surface data for a 20-year climatology (2c).

Figure 3: The diurnal cycle of summertime precipitation over the US with resolution 2.5° longitude by 2.0° latitude based on satellite data for 1999 (3a), surface data for 1999 (3b), and surface data for a 20-year climatology (3c). The diurnal amplitude is denoted by the color contour and also by the length of the arrow (see key on inset) (the same thereafter). The diurnal phase can be determined from the orientation of the arrows with respect to a 24-hour clock. Arrows pointing upward indicate a peak at 0000 LST (midnight), downward indicate a peak at 1200 LST (noon), towards the right indicate a peak at 0600 LST (dawn), and towards the left a peak at 1800 LST (sunset) (the same thereafter).

Figure 4: The diurnal cycle of summertime precipitation over NA at spatial resolution 0.1° longitude by 0.1° latitude based on satellite data for 1999. Note, for clarity, the arrows are plotted every 7 pixels with the arrows greater than 4 mm day^{-1} treated as 4 mm day^{-1} and the arrows lesser than 0.5 mm day^{-1} omitted.

Figure 5: The diurnal cycle of summertime precipitation over the Rocky Mountains and the Great Plains. Note, for clarity, the arrows are plotted every 3 pixels with the arrows greater than 6 mm day^{-1} treated as 6 mm day^{-1} and the arrows lesser than 0.5 mm day^{-1} omitted.

Figure 6: The Hovmöller diagram of the satellite radiances over the Rocky Mountains and the Great Plains (averaged over 40−41ºN) for 10−15 June 1999. Note the Continental Divide is located around 106ºW. The day of the month is in Mountain Standard Time (MST). For example, 0.00 indicates 0000 MST (midnight), 0.25 indicates 0600 MST (dawn), 0.50 indicates 1200 MST (noon), and 0.75 indicates 1800 MST (sunset).

Figure 7: The summertime mean precipitation (7a) and its diurnal cycle (7b) over the core NAM region. Note, for clarity, the arrows are plotted every 3 pixels with the arrows greater than 6 mm day^{-1} treated as 6 mm day^{-1} and the arrows lesser than 0.5 mm day^{-1} omitted.

Figure 8: The diurnal cycle of summertime precipitation over the mouth of the Gulf of California. Note, the arrows are plotted every pixel with the arrows greater than 6 mm day^{-1} treated as 6 mm day^{-1} and the arrows lesser than 0.5 mm day^{-1} omitted.

Figure 9: The Hovmöller diagram of the satellite radiances over the mouth of the GC (averaged over 21.5−22.5ºN) for 5−10 August 1999. Note the coastline is located around 105.5ºW.

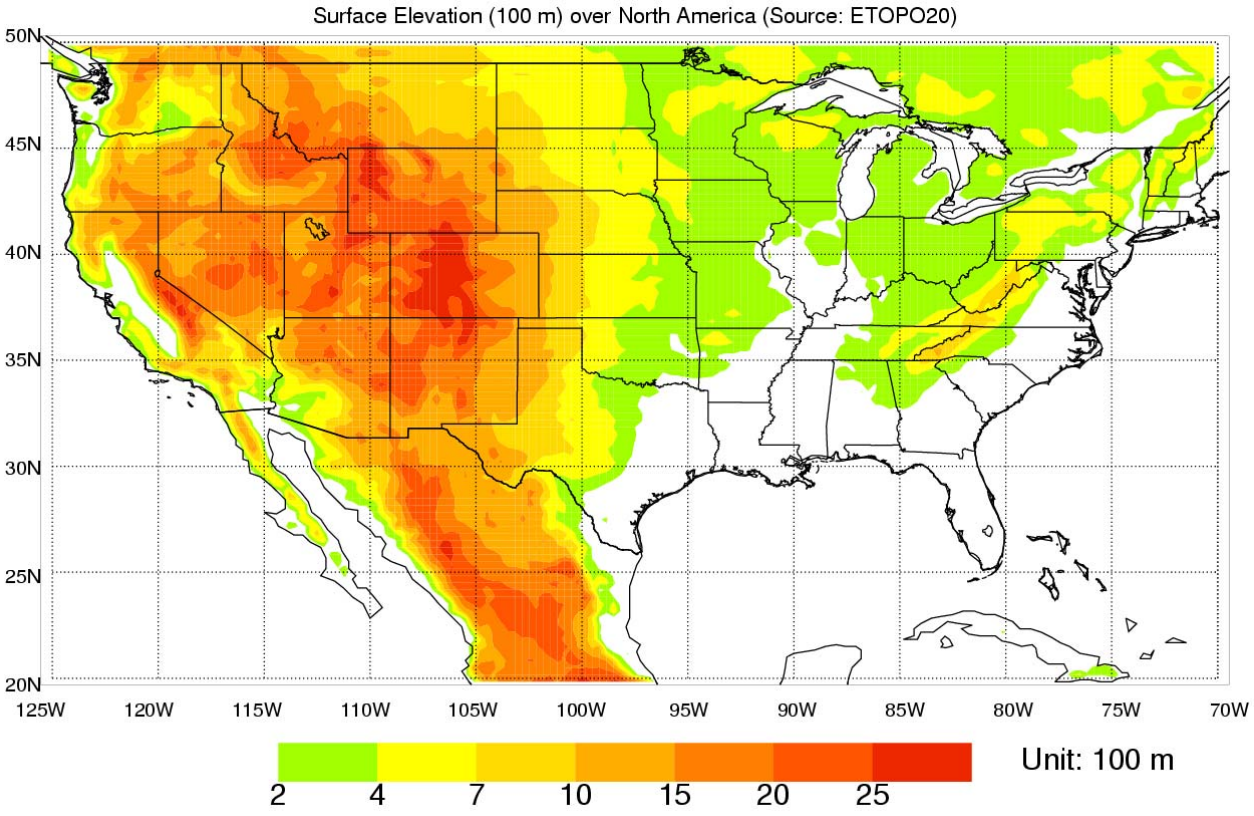

Figure 1: The 20-minute surface elevation over NA

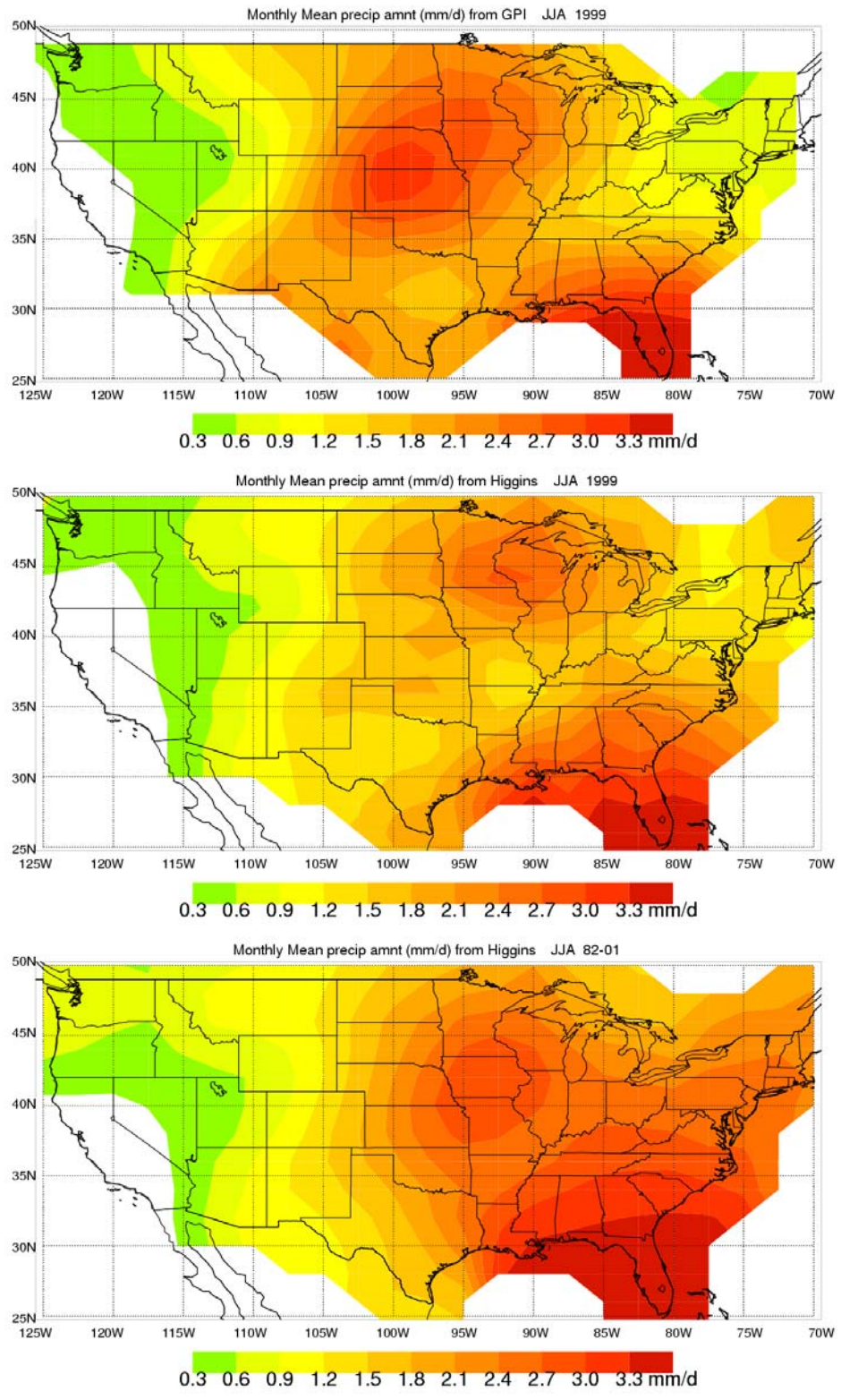

Figure 2: The summertime mean precipitation over the US with resolution 2.5° longitude by 2.0° latitude based on satellite data for 1999 (2a), surface data for 1999 (2b), and surface data for a 20-year climatology (2c).

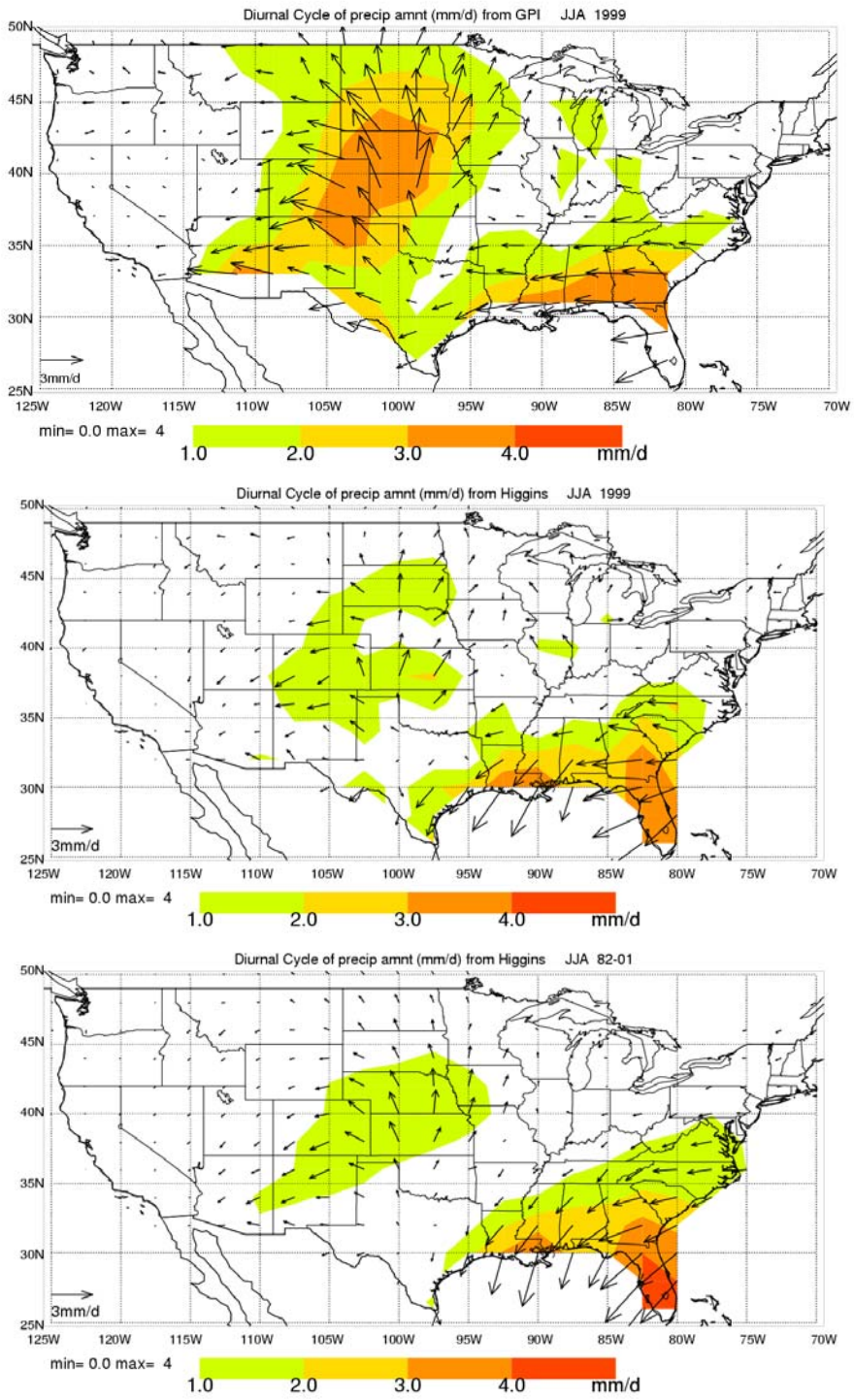

Figure 3: The diurnal cycle of summertime precipitation over the US with resolution 2.5° longitude by 2.0° latitude based on satellite data for 1999 (3a), surface data for 1999 (3b), and surface data for a 20-year climatology (3c). The diurnal amplitude is denoted by the color contour and also by the length of the arrow (see key on inset) (the same thereafter). The diurnal phase can be determined from the orientation of the arrows with respect to a 24-hour clock.

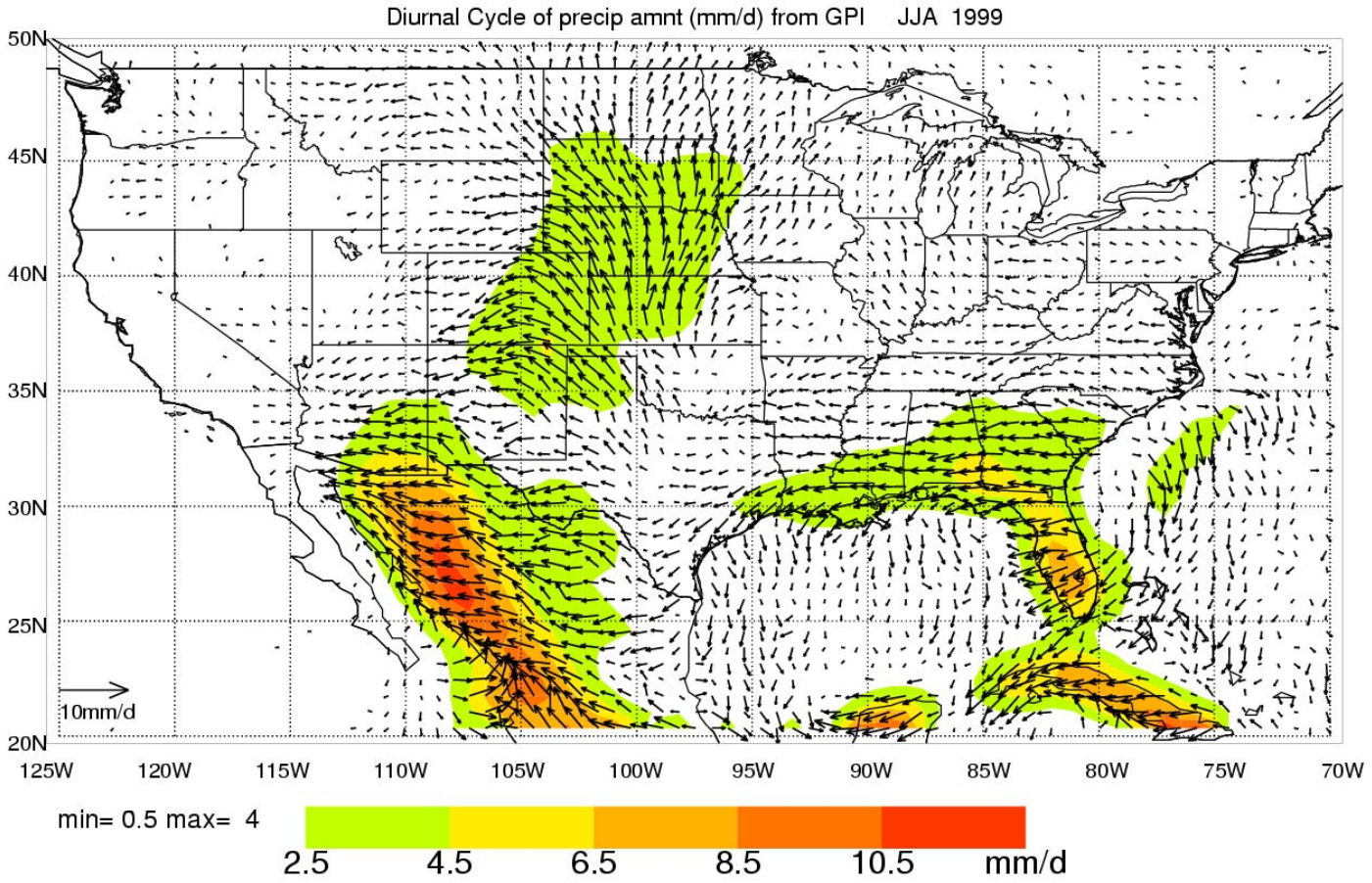

Figure 4: The diurnal cycle of summertime precipitation over NA at the spatial resolution 0.1°x0.1° longitude-latitude based on satellite data for 1999. Note, for clarity, the arrows are plotted every 7 pixels with the arrows greater than 4 mm day^{-1} treated as 4 mm day^{-1} and the arrows lesser than 0.5 mm day^{-1} omitted.

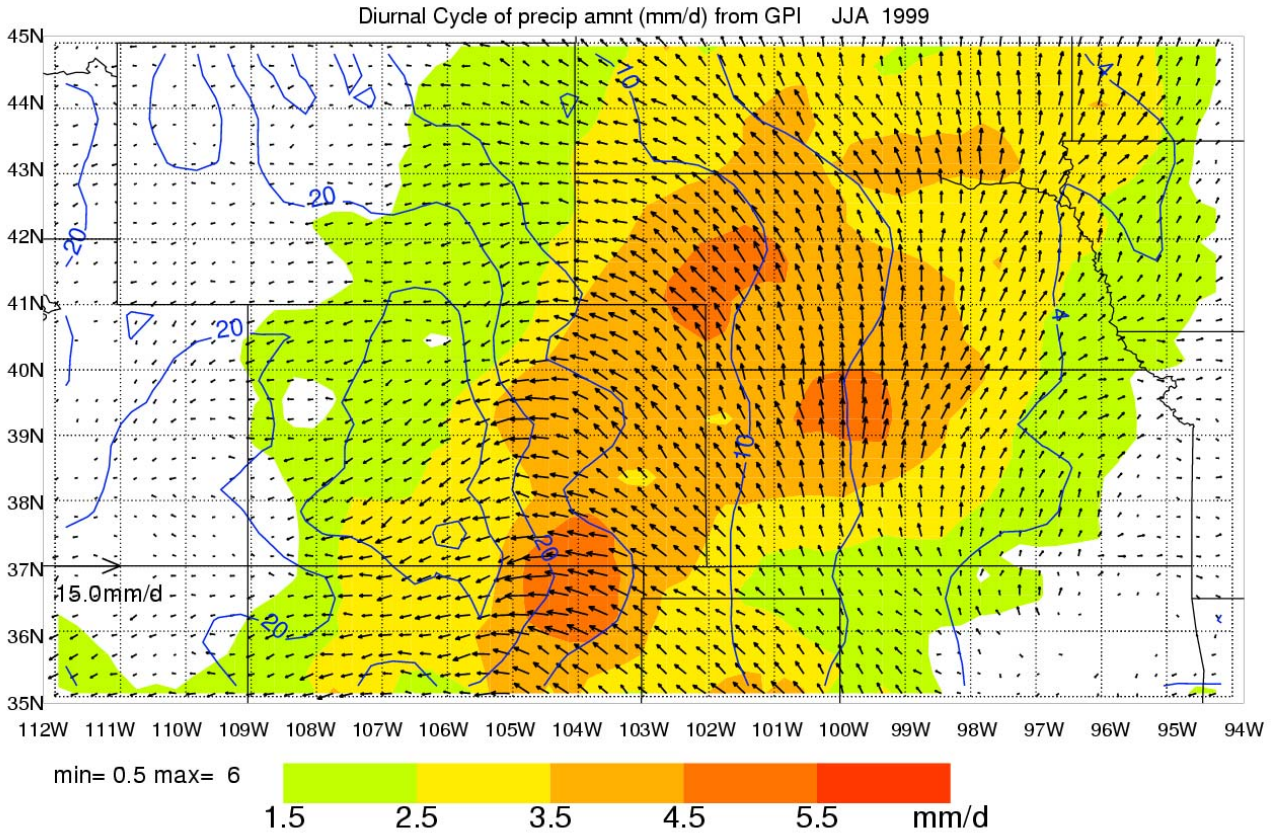

Figure 5: The diurnal cycle of summertime precipitation over the Rocky Mountains and the Great Plains. Note, for clarity, the arrows are plotted every 3 pixels with the arrows greater than 6 mm day^{-1} treated as 6 mm day^{-1} and the arrows lesser than 0.5 mm day^{-1} omitted.

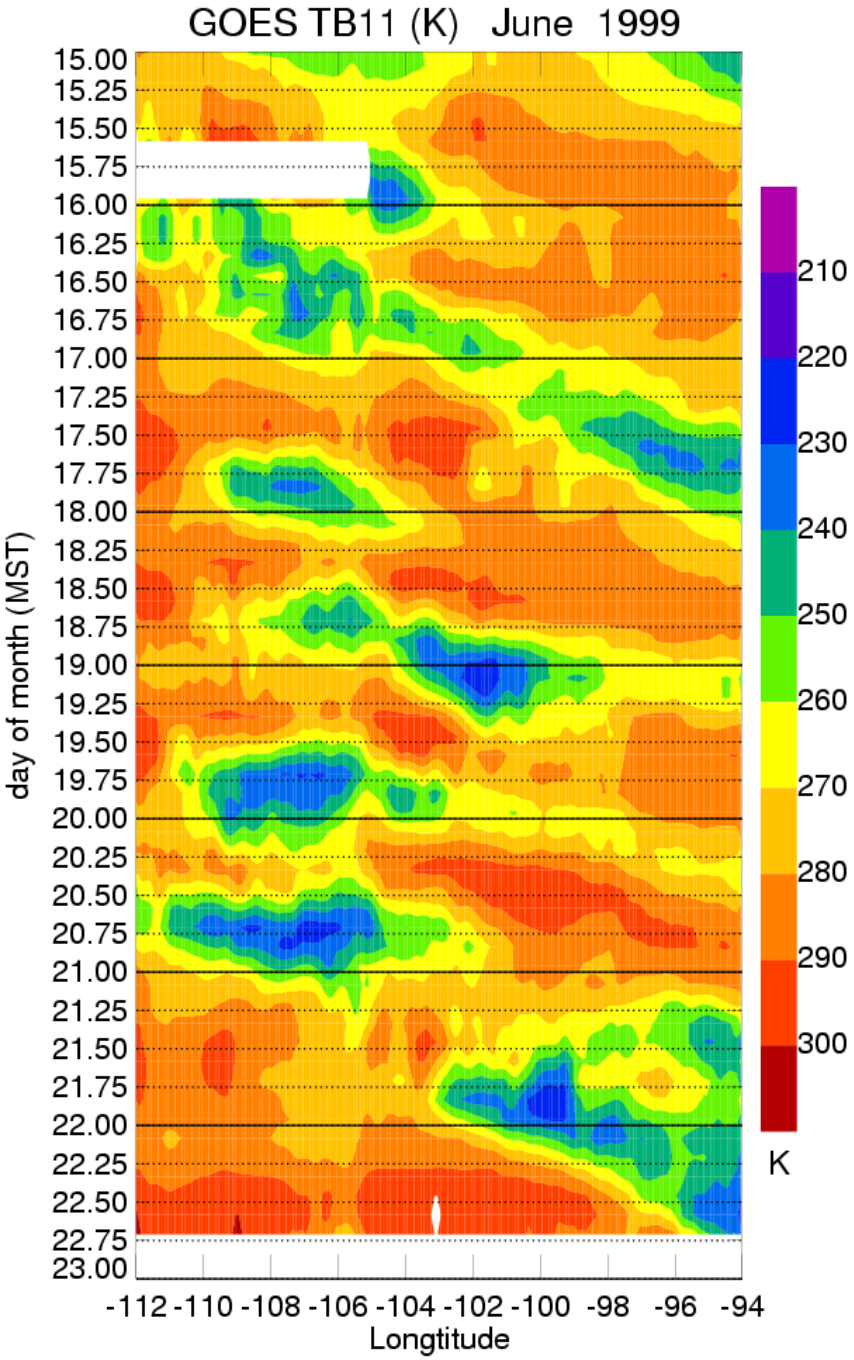

Figure 6: The Hovmöller diagram of the satellite radiances over the Rocky Mountains and the Great Plains (averaged over 40−41ºN) for 15−30 June 1999. Note the Continental Divide is located around 106ºW. The day of the month is in Mountain Standard Time (MST). For example, 0.00 indicates 0000 MST (midnight), 0.25 indicates 0600 MST (dawn), 0.50 indicates 1200 MST (noon), and 0.75 indicates 1800 MST (sunset).

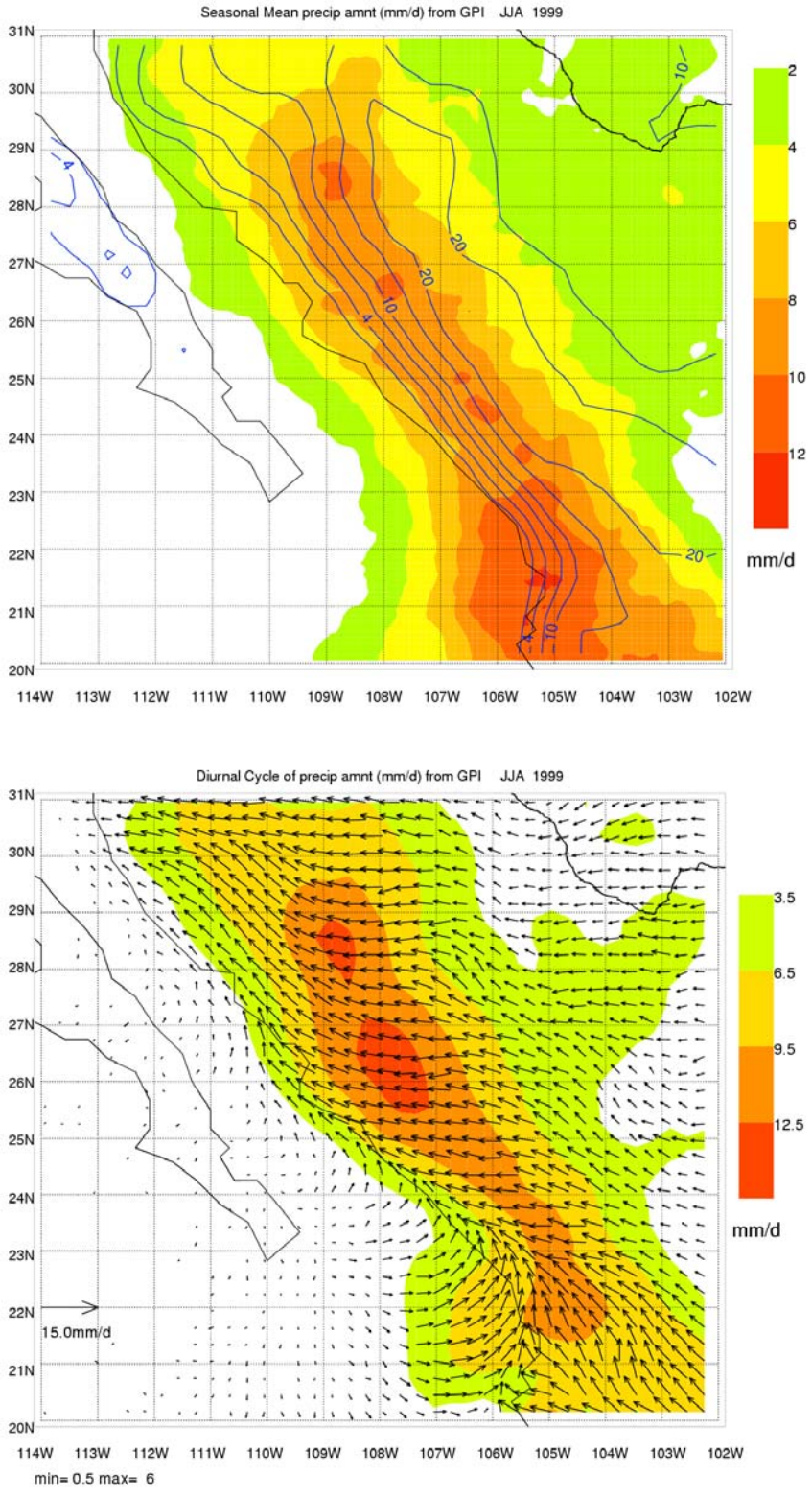

Figure 7: The summertime mean precipitation (7a) and its diurnal cycle (7b) over the core NAM region. Note, for clarity, the arrows are plotted every 3 pixels with the arrows greater than 6 mm day^{-1} treated as 6 mm day^{-1} and the arrows lesser than 0.5 mm day^{-1} omitted.

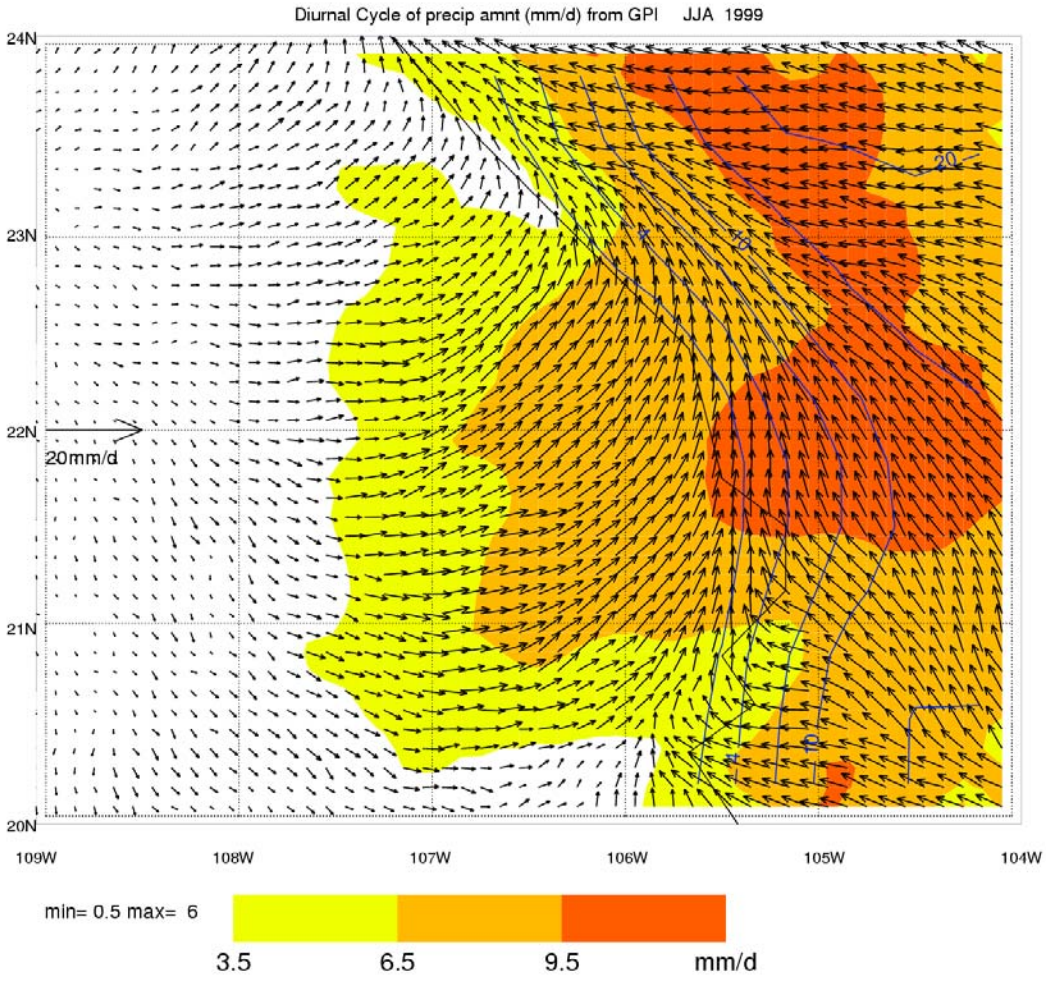

Figure 8: The diurnal cycle of summertime precipitation over the mouth of the Gulf of California. Note, the arrows are plotted every pixel with the arrows greater than 6 mm day^{-1} treated as 6 mm day^{-1} and the arrows lesser than 0.5 mm day^{-1} omitted.

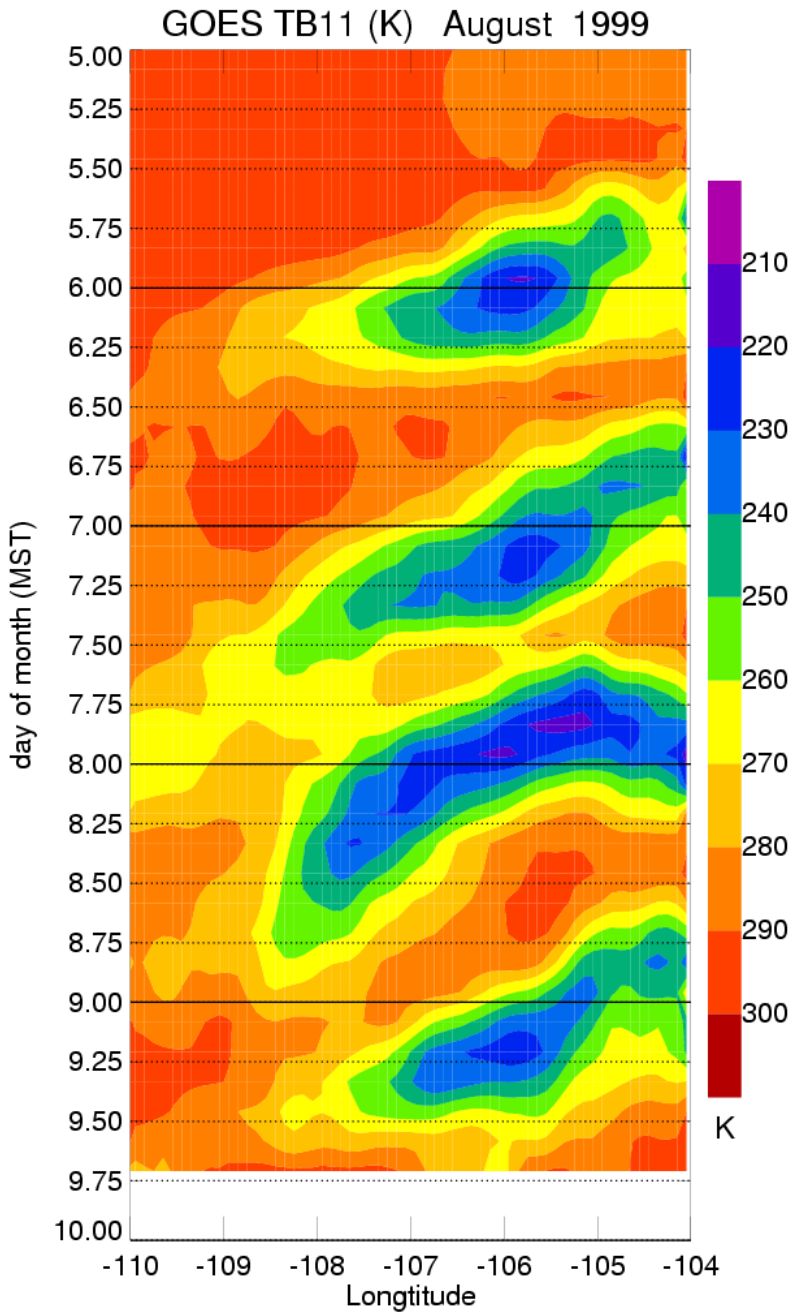

Figure 9: The Hovmöller diagram of the satellite radiances over the mouth of the GC (averaged over 21.5–22.5ºN) for 5–10 August 1999. Note the coastline is located around 105.5ºW.